

Supplementary Information

Table S1. Twelve target proteins for the two MRM experiments

Protein name	IPI accession number	Method	Probability of ProteinProphet	Number of unique peptides	Total number of peptides	Group	Used for 1st MRM	Used for 2nd MRM
Thyroxine-binding globulin precursor	IPI00292946	LTQ	1	21	56	A	○	○
Glyceraldehyde-3-phosphate dehydrogenase	IPI00219018	LTQ	1	5	12	A	○	○
Peroxiredoxin-2	IPI00027350	LTQ	1	6	8	A		○
gamma-Glutamyl hydrolase precursor	IPI00023728	LTQ	1	5	6	A	○	○
Myocilin precursor	IPI00019190	LTQ	1	5	5	A		○
Coagulation factor IX precursor	IPI00296176	LTQ	0.9	1	3	A		○
Kallistatin precursor	IPI00328609	LTQ	1	3	3	A	○	○
Hepatocyte growth factor activator precursor	IPI00029193	LTQ	1	2	2	A	○	○
von Willebrand factor precursor	IPI00023014	LTQ	1	3	3	A	○	○
Haptoglobin precursor	IPI00641737	LTQ	1	18	363	B		○
Apolipoprotein B-100 precursor	IPI00022229	LTQ	1	36	43	B		○
Pigment epithelium-derived factor precursor	IPI00006114	MALDI<Q	1	62	308	E		○

Two independent methods, ESI-MS/MS (LTQ LC-MS/MS, Thermo Fisher Scientific) and MALDI-MS/MS (4700 MALDI-TOF/TOF, Applied Biosystems), were used to profile the PDR vitreous proteome¹. The column ‘Method’ indicates the methods that were used to identify the proteins. The proteomic data were applied to the Trans-Proteomic Pipeline (TPP) to eliminate proteins that had low probabilities². The probability values are listed in the column ‘Probability of ProteinProphet.’ The column ‘Group’ refers to the groups in the Venn diagram in Supplementary Figure S1.

Table S2. Determination of rolling collision energy

Charge State	Slope	Intercept
2	0.050	5
3	0.044	3
4	0.05	2

$$\text{Collision Energy} = \text{Slope} \times [m/z] + \text{intercept}$$

When the charge state is confirmed in the ER (Enhanced Resolution) mode, the collision energy, which is applied to the precursor ion to produce its fragment ions, is determined using the equation (collision energy = (slope) x (m/z) + (intercept)). This equation for collision energy is optimized for triple quadrupole LC-MS/MS (4000 Q-Trap MS/MS, Applied Biosystems).

Figure S1

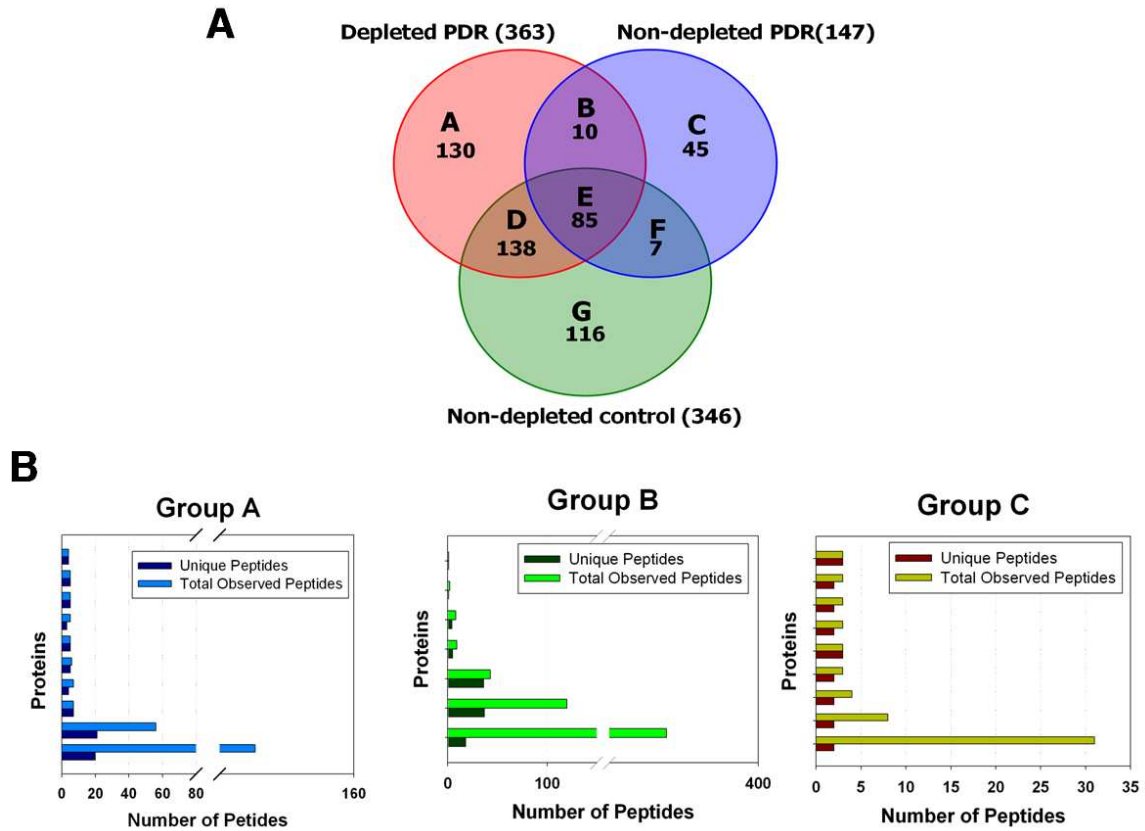


Figure S1. Groups of proteins in decreasing order of observed and unique peptide counts

(A) The candidate proteins that are specific to PDR vitreous were reported compared with MH vitreous¹. Candidate proteins that are specific to PDR vitreous correspond to the regions A, B, and C in the Venn diagram, and region G indicates MH-specific proteins. The Venn diagram represents the total numbers of identified proteins in each group. (B) Candidate proteins that are specific for PDR vitreous, extracted from plasma from Groups A, B, and C, were ordered by frequency of both unique and observed peptides. The numbers of observed peptides and unique

peptides for the listed proteins were plotted by decreasing number of total observed peptides.

Among the listed proteins in A, B, and C, 12 target proteins were selected for 2 MRM experiments, as summarized in Table S1. The X-axis shows the numbers of peptides, and the Y-axis indicates individual candidate proteins that are specific for PDR vitreous that belong to Group A, B, or C.

Figure S2

788 A-P-L-D-N-D-I-G-V-S-E-A-T-R 801

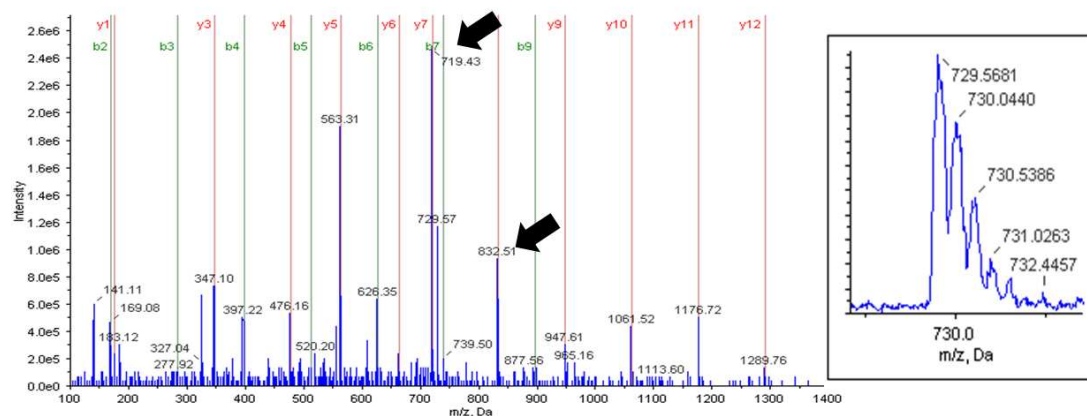


Figure S2. An example of the transition determination using Information-Dependent Analysis (IDA)

The Q1/Q3 transition of 729.5/719.4 m/z for a β -galactosidase peptide (residues 788–801, APLDNDIGVSEATR) was determined using the IDA method. One hundred femtomoles of peptide was analyzed by enhanced mass scan (EMS, survey scan) and 3 enhanced product ion scans (EPI, MS/MS scan). An MS/MS spectrum is shown in the left panel, and the peaks of the EMS scan (precursor ion at 729.5 m/z for residues APLDNDIGVSEATR) are shown in the right panel. The MS/MS spectra were used to identify β -galactosidase using the ProteinPilot program (version 2.0.1) and SwissProt (Release 54, July 2007). In the MS/MS spectrum, the highest and second-highest intensities of the fragment ions near the precursor ion mass are shown as 2 arrows, one of which is the Q1/Q3 transition of 729.5/719.4 m/z in the left panel.

Figure S3

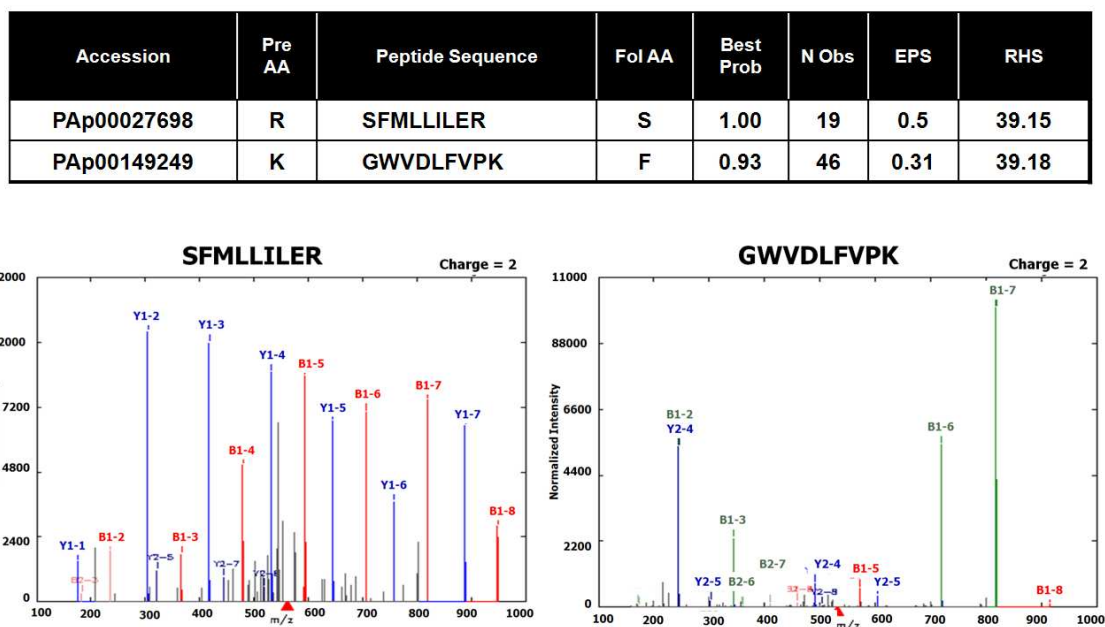


Figure S3. An example of the transition determination using the PeptideAtlas database

The transition of TBG was determined using the PeptideAtlas database (<http://www.PeptideAtlas.org>). The MS/MS spectrum, the information on m/z , and the intensity of the particular spectrum were obtained from the PeptideAtlas database. We selected target transitions using commonly suggested candidate transitions from the PeptideAtlas database and the MIDAS workflow. The MS/MS spectra for 2 precursor peptides (SFMLLILER and GWVDFVFPK) are shown with ion types in the bottom panels, and their Q1/Q3 transitions are listed in Table 2 of the text. The column ‘Accession’ represents the PeptideAtlas accession number, which begins with PAP and is followed by 9 digits; the columns ‘Pre AA’ and ‘Fol AA’

indicate “the amino acid which is preceding towards the N terminus” and “the amino acid which is following towards the C-terminus”. The column ‘Best Prob’ represents the highest PeptideProphet probability from the Trans-Proteomic Pipeline² for this observed sequence, and the column ‘N Obs’ is the total number of observations in all modified forms and charge states. The column ‘EPS’ lists the empirical observability scores, and RHS indicates the SSRCalc (Sequence Specific Retention Calculator)-related hydrophobicity score.

Figure S4

```

KAL      LMRWNNLLRKRNFYKKLELHLPKFSISGSYVLDQILPRLGFTDLFSKWADLSGITKQQKL 357
A1AT     ITKFLENEDRR----SASLHLPKLSITGTLDKSVLGQLGKITKVFNSGADLSGVTEEAPL 351
TBG      LKKWNRLLQK*G----WVDLFVPKF*ISATYDLGATLLKMGIQHAYSENADFSGLTEDNGL 344
LS3P     SSGRRPLEQQQ-----PHHIP--TSAPVYQQPQQQPVAQSYGGYKEPAAPVSIQR-SAP 200
          :          .:* : : *          :.: * .: .

KAL      EASKSFHKATLDVDEAGTEAAAATTFAIKFFSAQTNRH-ILRFNRPFLLVVFSTSTQSVL 416
A1AT     KLSKAVHKAVLTIDKKGTEAAGAMFLEAIPMSIPP----EVKFNKPFVFLMIEQNTKSPL 407
TBG      KLSNAAHKAVLHIGKEGTEAAAVPEVELSDQPENTFLHPPIQIDR*FMLLILE*STRSIL 404
LS3P     GGGGKRYRAVYDYSAADEDEVSFQDGDITVN-----VQQIDDGWMYGTVERTGDTGM 252
          . :.*. . . : ..          ::: :. . . : :

```

Figure S4. Sequence alignment of homologous proteins to thyroxine-binding globulin

The sequence of TBG was inputted into the BLAST program using a human proteome database (NCBI, <http://www.ncbi.nlm.nih.gov/BLAST/Blast.cgi>; database, SwissProt; organism, human (taxid: 9606); algorithm, protein-protein BLAST (blastp)), resulting in 3 homologous proteins: kallistatin (KAL, NCBI accession number: AAC41706), alpha-1-antitrypsin (A1AT, NCBI accession number: CAJ15161), and LIM and SH3 protein 1 (LS3P, NCBI accession number: NP_006139). The sequences of these proteins were aligned with TBG using the CLUSTALW algorithm (<http://www.ebi.ac.uk/Tools/clustalw2/index.html>). Two dotted boxes indicate the 2 precursor peptides of the Q1 transitions, which were selected based on the PeptideAtlas database. The aligned sequences show that the 2 selected peptides are specific for TBG among the 3 homologous proteins. The numbers represent the amino acid residues, and “*” in the bottom line denotes an identical, conserved residue, and “:” and “.” stand for the amino acid that shows similarity.

Figure S5

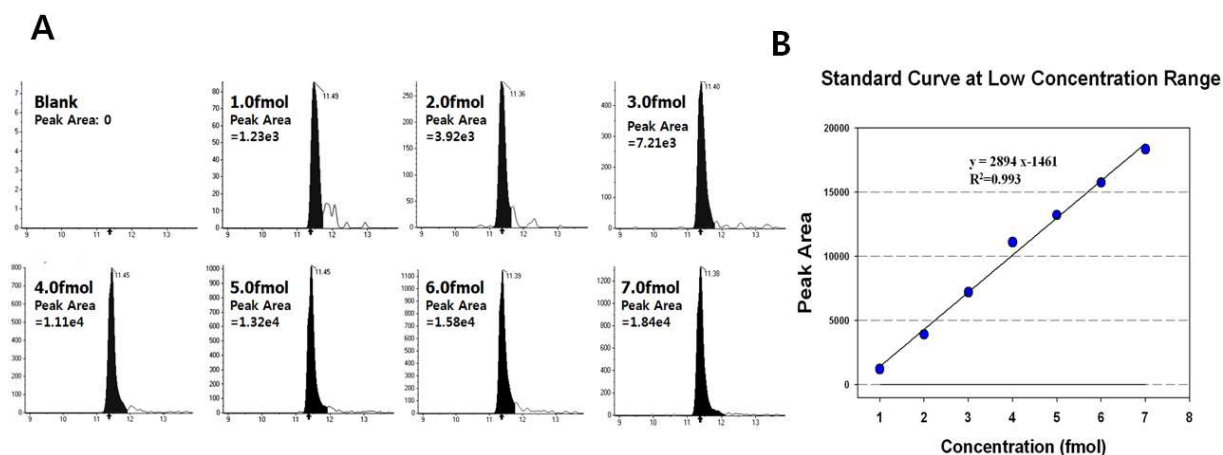


Figure S5. The second standard curve of beta-galactosidase peptide at the low concentrations

The standard curve in the low-concentration range was determined for the transition for beta-galactosidase peptide (GDFQFNISR) at 542.3/636.3 m/z using the IDA method. (A) The concentration points were 1.0, 2.0, 3.0, 4.0, 5.0, 6.0, and 7.0 fmol including the blank. The peak area for each MRM run was extracted and calculated. (B) The R^2 value of linearity is 0.993, showing good correlation between the concentration and intensity.

Figure S6

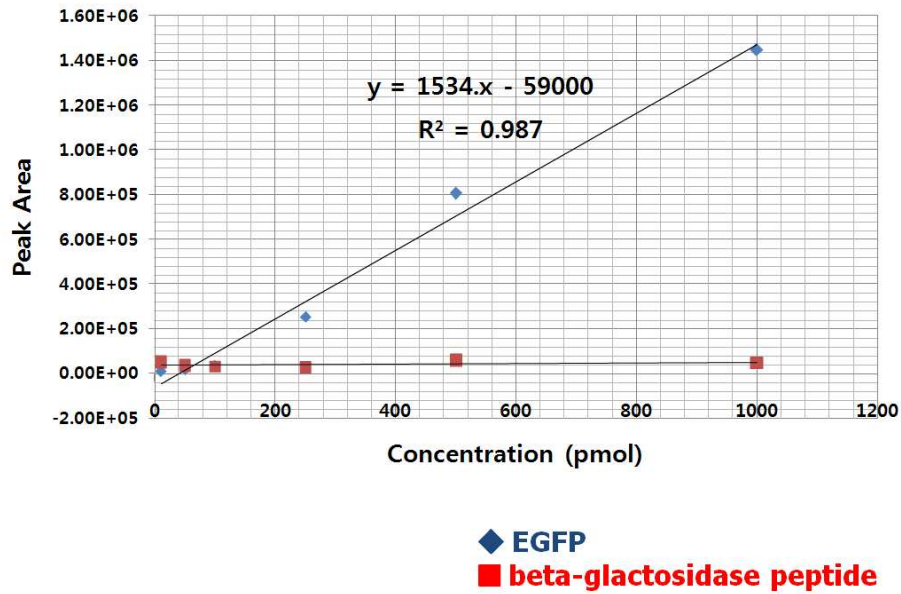


Figure S6. The measurement of the relative concentration for exogenous protein (EGFP) in plasma using the standard curve of beta-galactosidase

The relative concentration of spiked exogenous EGFP in plasma was determined versus beta-galactosidase using the standard curve for beta-galactosidase. Purified EGFP was spiked into plasma at 0, 10, 50, 100, 250, 500, and 1000 pmol, followed by in-solution digestion and desalting. After the internal standard peptide was added (100 fmol of beta-galactosidase peptide GDFQFNISR), MRM was performed for the EGFP (525.8/774.4 m/z) and beta-galactosidase transitions (542.3/636.3 m/z). The resulting concentration curve had an R^2 value of 0.987 versus the intensities with good linearity.

Figure S7

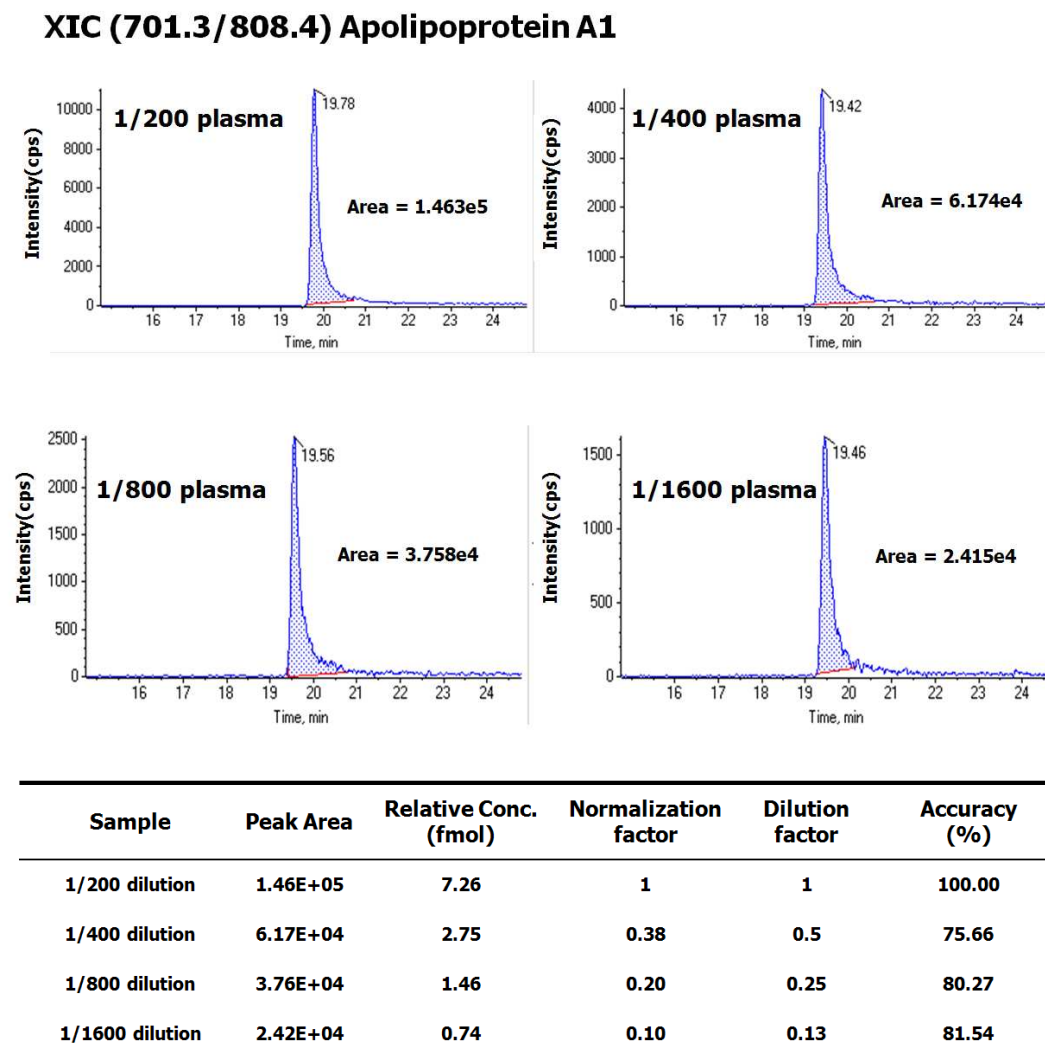


Figure S7. Extrapolation of serially diluted apolipoprotein A1 onto the standard curve

The plasma sample containing apolipoprotein A1 was serially diluted (1/200, 1/400, 1/800, and 1/1600). MRM runs were performed to measure the Q1/Q3 transitions of apolipoprotein A1 in the 4 diluted plasma samples using the XIC (701.3/808.4 m/z). The Q1/Q3 transition of apolipoprotein A1 was predetermined using the IDA method. One hundred femtomoles of the

beta-galactosidase peptide standard (residues 954-962, GDFQFNISR) was added to the 4 diluted plasma samples for normalization, as shown in Figure 4. The peak areas of the extracted ion chromatogram (XIC:701.3/808.4) were measured and compared with that of the 1/200 dilution to examine the measurement accuracy in the 4 serially diluted apolipoprotein A1 samples. In brief, the relative amount of apolipoprotein A1 in the 1/200 dilution was extrapolated onto the standard curves of beta-galactosidase, which resulted in a concentration of 7.26 fmole. Subsequently, 'Relative Concentration' and 'Normalization Factor' were calculated in the other 3 dilutions to represent the ratios against the concentration of apolipoprotein A1 in the 1/200 dilution. The column 'Dilution Factor' represents the theoretical dilution factor of apolipoprotein A1 in each dilution. The ratio of 'Normalization Factor' represents experimentally measured concentrations in each MRM run versus that of the 1/200 dilution. The accuracies of the measurements (normalization factor/dilution factor) were 75.66%, 80.27%, and 81.54% at the 1/400, 1/800, and 1/1600 dilutions versus the 1/200 dilution, respectively.

Figure S8

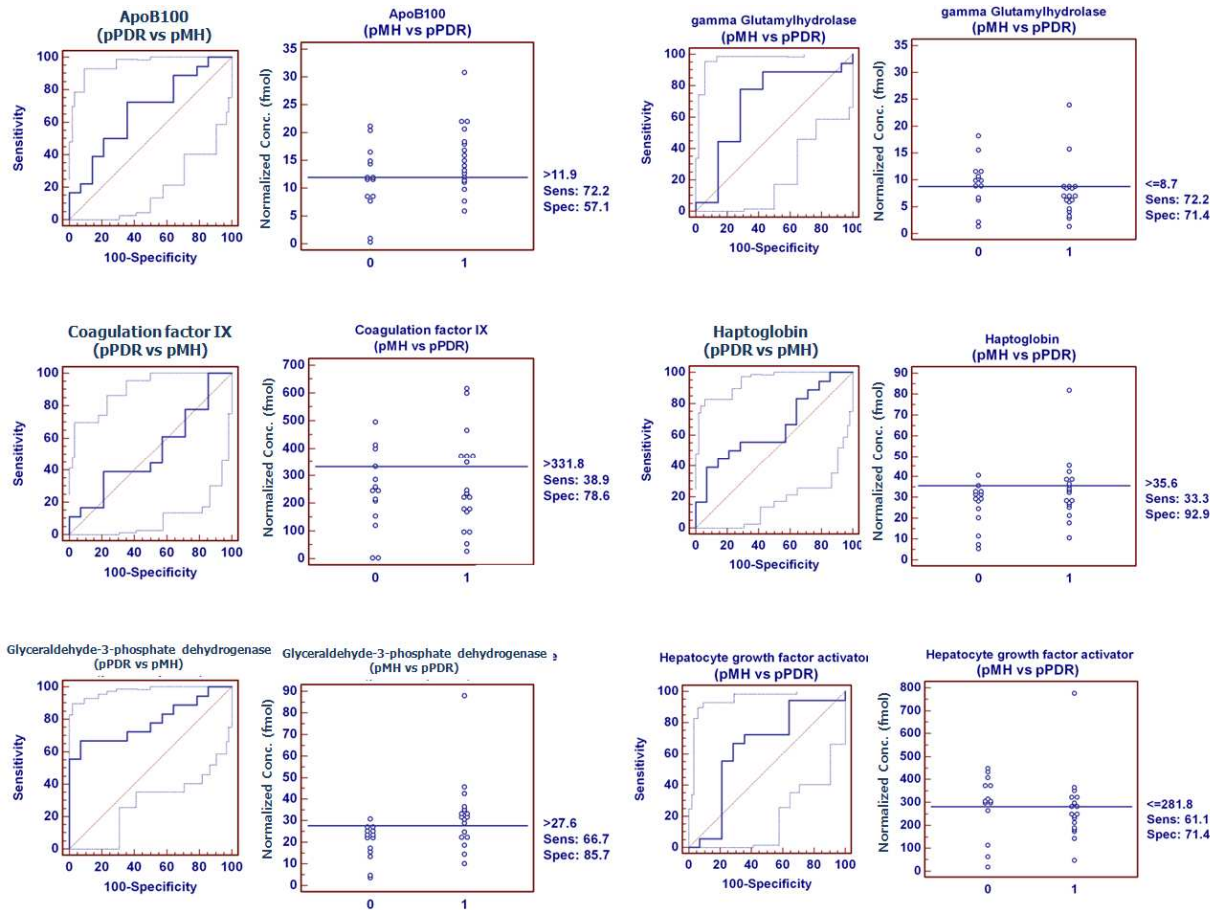


Figure S8 (Continued)

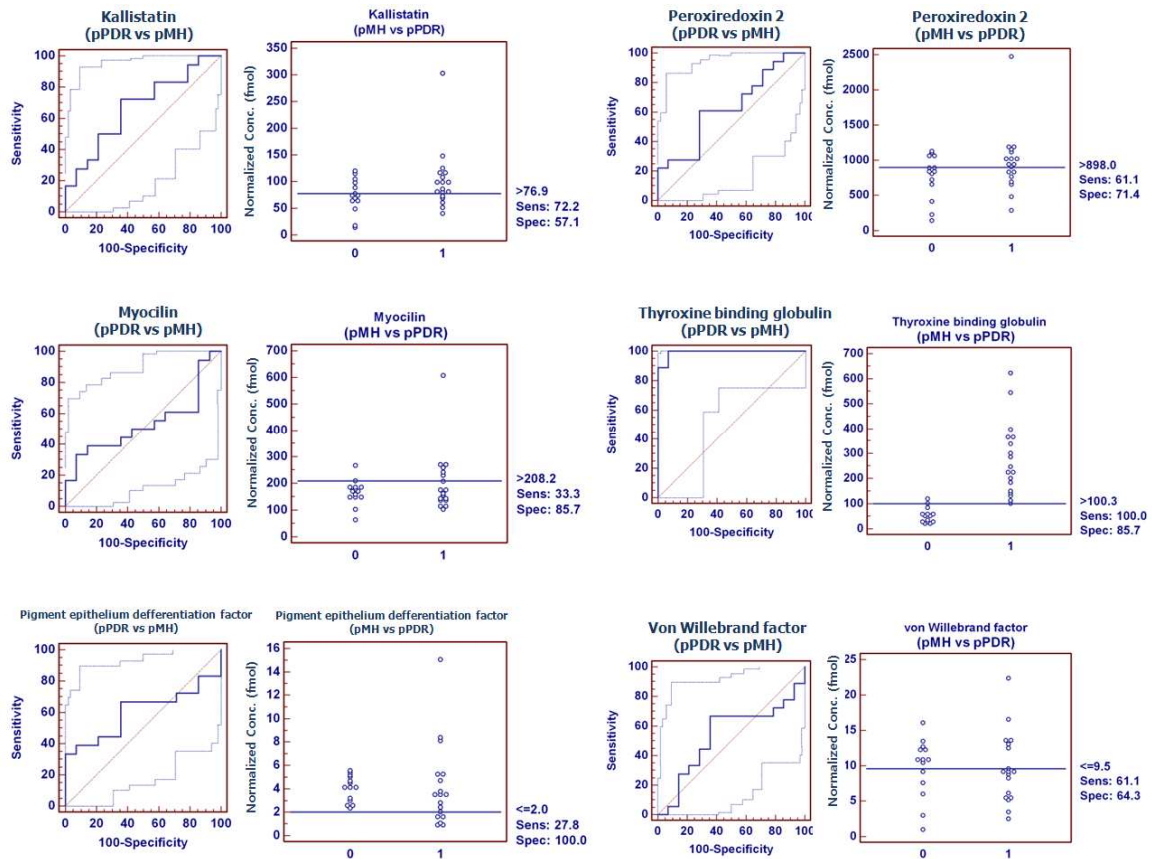


Figure S8. ROC curves and interactive plots of MRM in PDR versus MH plasma

pMH and pPDR represent MH and PDR plasma, respectively. In the ROC curve, the solid line indicates the corresponding value in sensitivity and 100-specificity. In the interactive plot, the Y-axis represents the normalized concentration of the target protein against the standard curve of the beta-galactosidase peptide. The sensitivity and specificity at the cutoff concentration are indicated on the right side of the interactive plot. Group 0 represents MH, and Group 1 indicates

PDR plasma. If the target protein concentration in PDR plasma decreased compared with MH (for example, gamma glutamyl hydrolase), the ROC curve was inversely plotted (pMH versus pPDR).

Figure S9

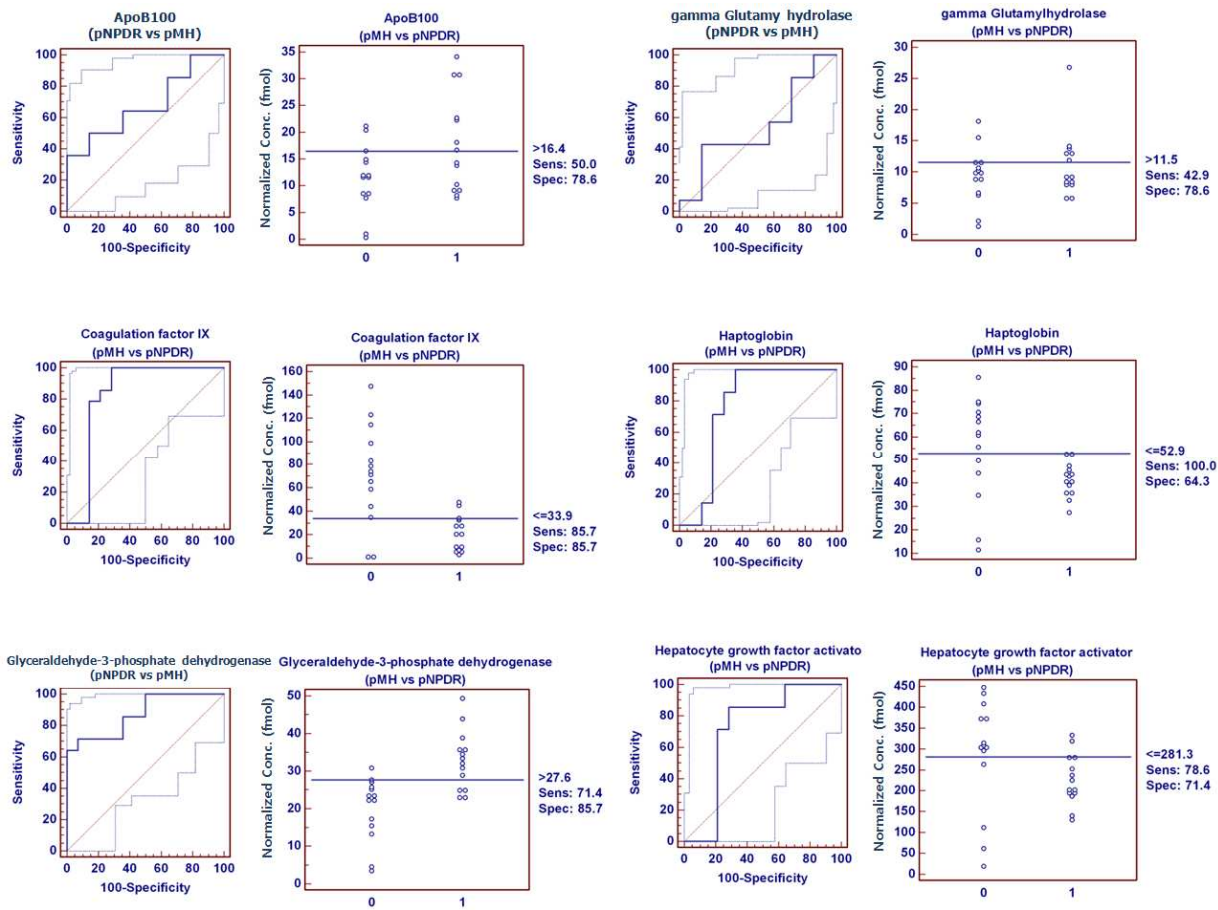


Figure S9 (Continued)

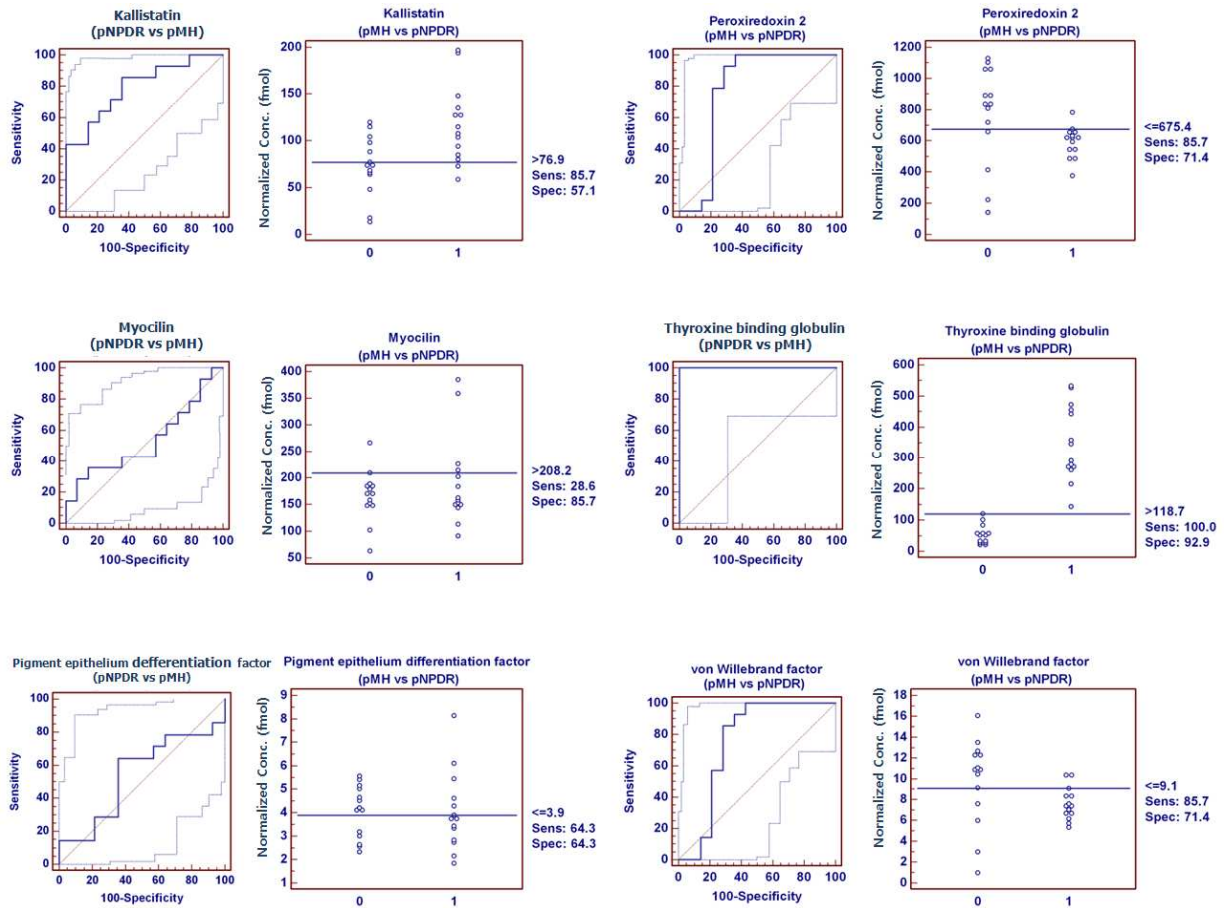


Figure S9. ROC curves and interactive plots of MRM in NPDR versus MH plasma

pMH and pNPDR represent MH and NPDR plasma, respectively. Group 0 represents MH, and Group 1 indicates NPDR plasma. If the target protein concentration in NPDR plasma decreased compared with MH (for example, haptoglobin), the ROC curve was inversely plotted (pMH versus pNPDR). The other details are the same as Figure S8.

Figure S10

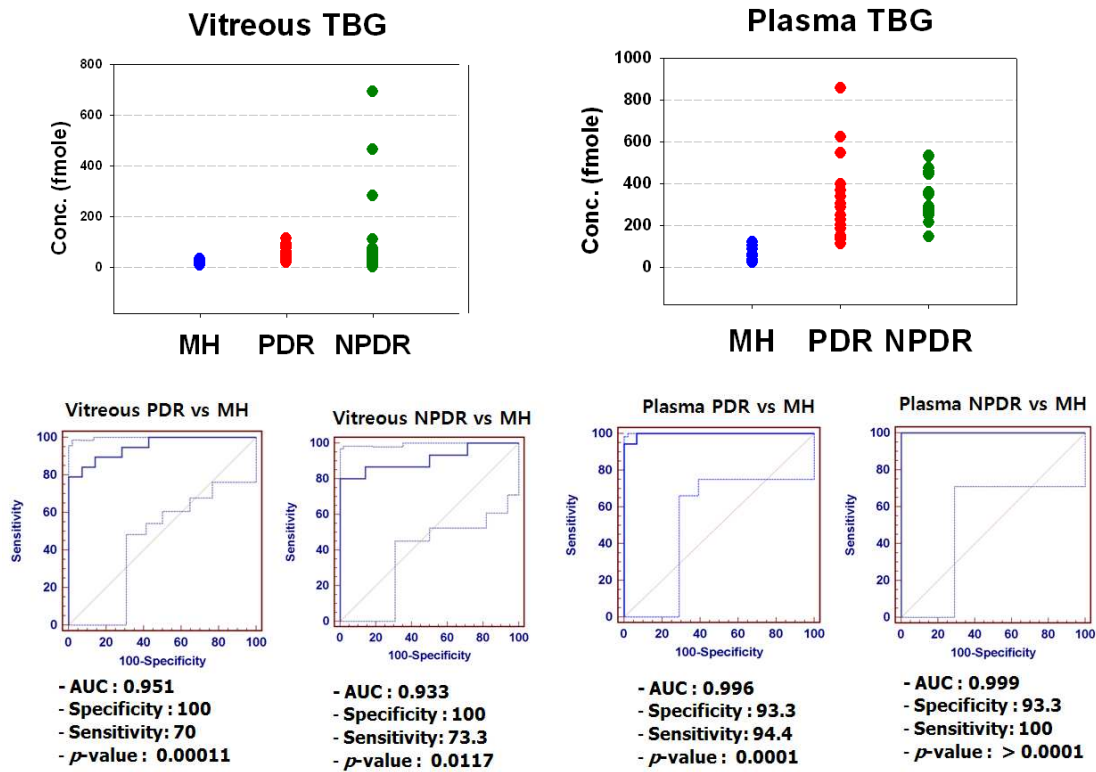
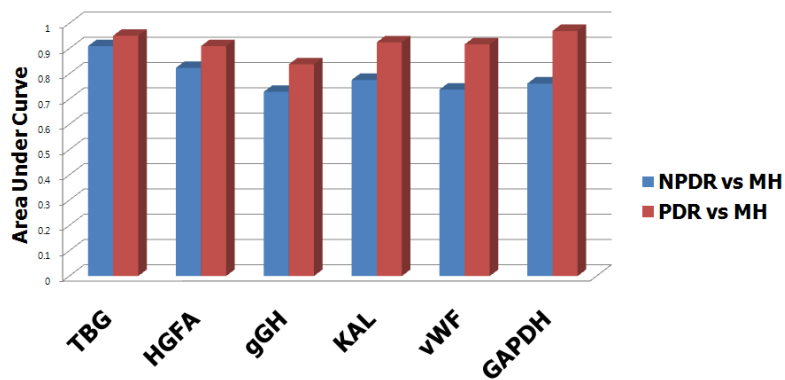


Figure S10. Interactive plots and ROC curves of thyroxine-binding globulin in vitreous and plasma

Relative concentrations of vitreous and plasma TBG in MH, PDR, and NPDR were plotted in the interactive plots and ROC curves, based on the extrapolated concentration onto the standard curve. MH, PDR, and NPDR are indicated as blue, red, and green circles, respectively (upper panel). The ROC curves of TBG in both PDR and NPDR vitreous versus MH are drawn in the 2 lower-left panels, and those of TBG in both PDR and NPDR plasma versus MH are drawn in the 2 right panels. AUC values, specificity, sensitivity, and p -values are shown for each ROC curve. The figure legends are the same as in Figures 5-6 and Supplementary Figures S8-S9.

Figure S11

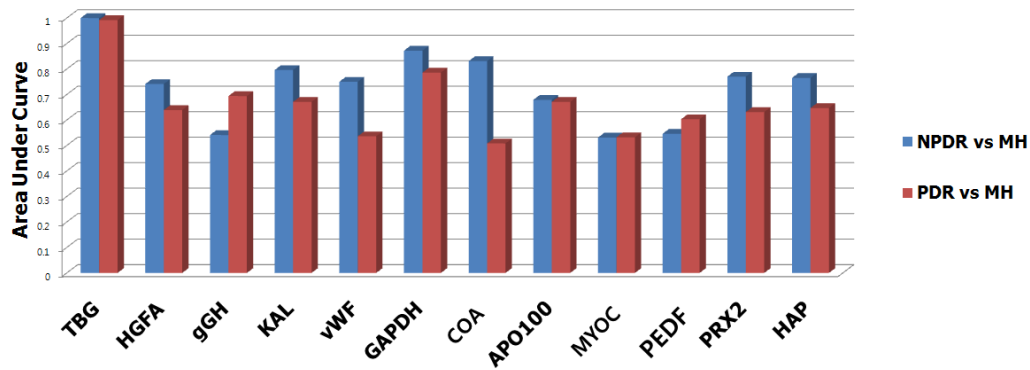


Group	TBG	HGFA	gGH	KAL	vWF	GAPDH
NPDR vs MH	0.91	0.824	0.729	0.776	0.738	0.762
PDR vs MH	0.951	0.91	0.838	0.925	0.917	0.97

Figure S11. Comparison of AUC values for 6 target proteins in the first MRM experiment

The AUC values of 6 target proteins in vitreous are plotted as bars. The Y-axis represents the AUC values, and the X-axis indicates the 6 proteins. The blue bars show the differences between NPDR and MH, and the red bars represent differences between PDR and MH.

Figure S12



Group	TBG	HGFA	gGH	KAL	vWF	GAPDH	COA	AP0100	MYOC	PEDF	PRX2	HAP
NPDR vs MH	1.000	0.741	0.541	0.796	0.75	0.872	0.831	0.679	0.531	0.546	0.77	0.765
PDR vs MH	0.992	0.639	0.694	0.671	0.536	0.786	0.508	0.671	0.532	0.603	0.631	0.647

Figure S12. Comparison of AUC values for 12 target proteins in the second MRM experiment

The AUC values of 12 target proteins in plasma are plotted as bars. The Y-axis represents the AUC values, and the X-axis indicates the 12 proteins. The blue bars show differences between NPDR and MH, and the red bars represent differences between PDR and MH. COA, APO100, MYOC, and PRX2 are coagulation factor IX, apolipoprotein B-100, myocilin, and peroxiredoxin 2, respectively.

Figure S13

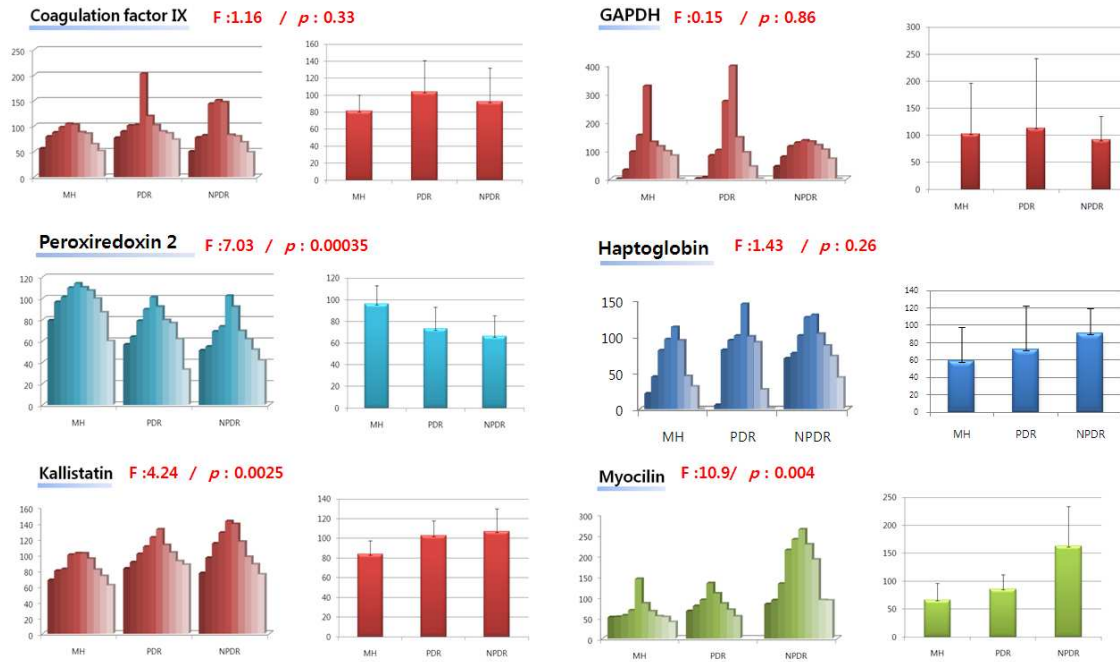


Figure S13. Western blot verification

Ten female and 10 male plasma samples in each group were used for Western blot of target proteins. The results of the Western blots were statistically analyzed for 6 proteins (coagulation factor XI, peroxiredoxin 2, kallistatin, GAPDH, haptoglobin, myocilin) using ANOVA between the MH, PDR, and NPDR groups. The intensity of Western blot bands was measured and normalized against the band intensity of pooled internal standard plasma. In the left panel, the normalized intensities of individual Western blot bands are plotted for the 3 groups, and average intensity (bar) and standard variation (line above the bar) are shown in the right panel. The red letters “F” and “p” represent the degree of freedom and the probability from ANOVA, respectively.

References

1. Kim, T.; Kim, S. J.; Kim, K.; Kang, U. B.; Lee, C.; Park, K. S.; Yu, H. G.; Kim, Y., Profiling of vitreous proteomes from proliferative diabetic retinopathy and nondiabetic patients. *Proteomics* **2007**, 7, (22), 4203-15.
2. Nesvizhskii, A. I.; Keller, A.; Kolker, E.; Aebersold, R., A statistical model for identifying proteins by tandem mass spectrometry. *Anal Chem* **2003**, 75, (17), 4646-58.